

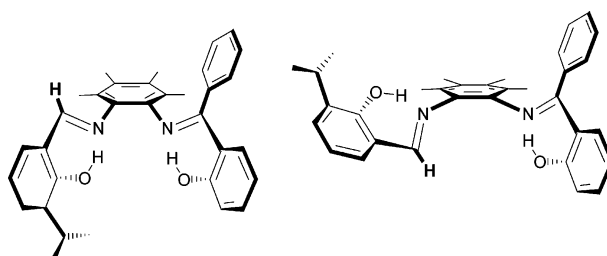
Stereomutations of Atropisomers of Sterically Hindered Salophen Ligands

Antonella Dalla Cort,[†] Francesco Gasparrini,^{*,‡} Lodovico Lunazzi,^{*,§} Luigi Mandolini,^{*,†} Andrea Mazzanti,[§] Chiara Pasquini,[†] Marco Pierini,[‡] Romina Rompietti,[‡] and Luca Schiaffino[†]

Dipartimento di Chimica and IMC-CNR Sezione Meccanismi di Reazione, Università La Sapienza, Box 34 Roma 62, 00185 Roma, Italy, Dipartimento di Studi di Chimica e Tecnologia delle Sostanze Biologicamente Attive, Università La Sapienza, Piazzale Aldo Moro 5, 00185 Roma, Italy, and Dipartimento di Chimica Organica "A Mangini", Università di Bologna, Viale Risorgimento 4, 40136 Bologna, Italy

francesco.gasparrini@uniroma1.it; lunazzi@ms.fci.unibo.it; luigi.mandolini@uniroma1.it

Received July 1, 2005



The stereomutations in nonsymmetrical salophen ligands **1–4** were studied by means of dynamic NMR and HPLC methods. DNMR experiments showed that in DMSO-*d*₆ hindered ligands **2–4** exist in two chiral conformations, depending on whether the imine carbon atoms are in a *cis* or *trans* disposition with respect to the plane of the central *o*-phenylenediamine ring, the latter being more stable by 1.0 kcal mol⁻¹. Owing to its higher dipole moment, in the apolar solvent C₆D₆ the *cis* conformer is destabilized with respect to the *trans* one, in agreement with the results of ab initio calculations. In DMSO-*d*₆ solution the two conformers are in equilibrium through the less hindered rotation about the C6–N7 bond aligned to the *a*_{6,7} axis, and the interconversion barriers range from 18.4 to 19.3 kcal mol⁻¹. The enantiomerization process is a two step-process that implies sequential rotations around the C6–N7 and the C1–N8 bonds, so that the rate determining step is the slower rotation around the more hindered C1–N8 bond aligned to the *a*_{1,8} axis, and the energy barriers range from 21.4 to 21.9 kcal mol⁻¹. These values compare well with those determined by chromatography on an enantioselective HPLC column at low temperature, thus confirming that DNMR and DHPLC can be conveniently employed as complementary techniques.

Introduction

Schiff bases are among the most popular ligands because of their ease of formation and rich coordination chemistry with a large variety of metal ions.¹ Condensa-

tion of a diamine such as ethylenediamine (*o*-phenylenediamine) with salicylaldehyde affords the tetradentate salen (salophen, Scheme 1) ligand featuring two neutral nitrogens and two easily ionizable hydroxyls located in a planar arrangement suitable for equatorial coordination to transition metals. Such complexes have found interesting applications in different areas, particularly in modeling the metal-containing sites in metalloenzymes² and in the asymmetric catalysis of synthetically useful organic reactions.³

[†] Dipartimento di Chimica and IMC-CNR Sezione Meccanismi di Reazione, Università La Sapienza.

[‡] Dipartimento di Studi di Chimica e Tecnologia delle Sostanze Biologicamente Attive, Università La Sapienza.

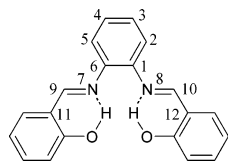
[§] Dipartimento di Chimica Organica "A Mangini", Università di Bologna.

(1) (a) Vigato, P. A.; Tamburrini, S. *Coord. Chem. Rev.* **2004**, *248*, 1717. (b) Hernandez Molina, R.; Mederos, A. Acyclic and Macrocyclic Schiff Base Ligands. In *Comprehensive Coordination Chemistry II From Biology to Nanotechnology*; McCleverty J. A., Meyer T. J., Eds.; Elsevier Pergamon Press: Amsterdam, 2004; Vol. 1, Chapter 19, pp 411–446. (c) Atwood D. A. *Coord. Chem. Rev.* **1997**, *165*, 267.

(2) (a) Santos, M. L. P.; Bagatin, I. A.; Pereira, E. M.; Ferreira, A. M. C. *J. Chem. Soc., Dalton Trans.* **2001**, 838. (b) Liu, S.-Y.; Nocera, D. G. *J. Am. Chem. Soc.* **2005**, *127*, 5278.

(3) (a) Cozzi, P. G. *Chem. Soc. Rev.* **2004**, *33*, 410. (b) Yamada, S. *Coord. Chem. Rev.* **1999**, *190–192*, 537.

SCHEME 1. Chemical Formula of the Parent Salophen Ligand, Showing Intramolecular Hydrogen Bonding to the Imine Nitrogens and Numbering of the Relevant Atoms Used throughout This Work



Salen and salophen ligands form neutral complexes with the uranyl dication UO_2^{2+} in which a fifth coordination site in the equatorial plane of the uranium is available for complexation with an additional monodentate ligand such as a hard anion or a neutral donor molecule. This property has promoted the use of uranyl salophen (salen) complexes as molecular receptors,⁴ catalysts,⁵ carriers,⁶ and sensors.⁷

In complexes with the uranyl dication, the salophen ligand is forced into a nonplanar, highly puckered conformation by the large radius of the uranium.^{8,9} Due to this structural feature, uranyl complexes of nonsymmetrically substituted salophen ligands have no symmetry elements and, in principle, should be amenable to resolution into enantiomeric forms.¹⁰ However, it was recently shown that the chirality of sterically unhindered complexes is labile because of a dynamic process. This process is a very fast conformational flip, which inverts the curvature through disrotatory motions around the C–N single bonds, as shown in eq 1. Bulky substituents in suitable positions slow considerably the flipping motion and make the chirality detectable. For example, the activation barrier for curvature inversion rises from 15.7 to 24.6 kcal mol⁻¹ on going from the uranyl complex of the phenyl-substituted ligand **1** to that of ligand **4** as a consequence of the methyl substituents in the *o*-phenylenediamine subunit.¹¹

(4) (a) van Doorn, A. R.; Bos, M.; Harkema, S.; van Eerden, J.; Verboom, W.; Reinhoudt, D. N. *J. Org. Chem.* **1991**, *56*, 2371 and references therein cited. (b) van Axel Castelli, V.; Dalla Cort, A.; Mandolini, L.; Pinto, V.; Reinhoudt, D. N.; Ribaud, F.; Sanna, C.; Schiaffino, L.; Snellink-Ruël, B. H. M. *Supramol. Chem.* **2002**, *14*, 211.

(5) (a) van Axel Castelli, V.; Cacciapaglia, R.; Chiosis, G.; van Veggel, F. C. J. M.; Mandolini, L.; Reinhoudt, D. N. *Inorg. Chim. Acta* **1996**, *246*, 181. (b) van Axel Castelli, V.; Dalla Cort, A.; Mandolini, L.; Reinhoudt, D. N. *J. Am. Chem. Soc.* **1998**, *120*, 12688. (c) van Axel Castelli, V.; Dalla Cort, A.; Mandolini, L.; Reinhoudt, D. N.; Schiaffino, L. *Chem. Eur. J.* **2000**, *6*, 1193. (d) van Axel Castelli, V.; Dalla Cort, A.; Mandolini, L.; Reinhoudt, D. N.; Schiaffino, L. *Eur. J. Org. Chem.* **2003**, 627 and references therein cited.

(6) Christoffels, L. A. J.; de Jong, F.; Reinhoudt, D. N. *Chem. Eur. J.* **2000**, *6*, 1376.

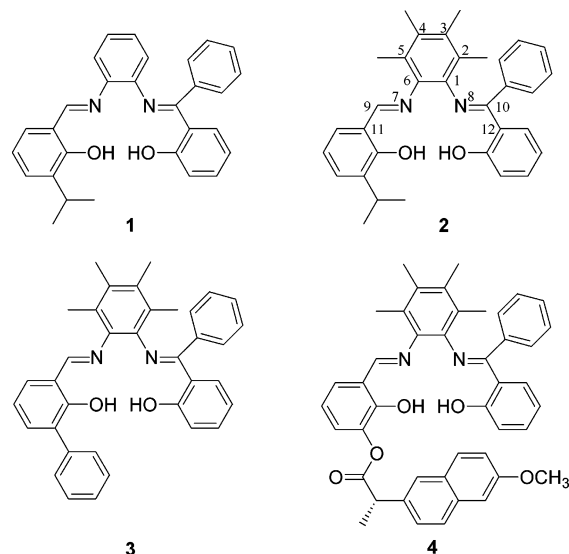
(7) Antonisse, M. M. G.; Snellink-Ruël, B. H. M.; Engbersen, J. F. J.; Reinhoudt, D. N. *J. Org. Chem.* **1988**, *53*, 9776.

(8) For X-ray structural studies, see: (a) van Staveren, C. J.; van Eerden, J.; van Veggel, F. C. J. M.; Harkema, S.; Reinhoudt, D. N. *J. Am. Chem. Soc.* **1988**, *110*, 4994. (b) van Doorn, A. R.; Schaafstra, R.; Bos, M.; Harkema, S.; van Eerden, J.; Verboom, W.; Reinhoudt, D. N. *J. Org. Chem.* **1991**, *56*, 6083. (c) Rudkevich, D. M.; Stauthamer, W. P. R. V.; Verboom, W.; Engbersen, J. F. J.; Harkema, S.; Reinhoudt, D. N. *J. Am. Chem. Soc.* **1992**, *114*, 9671. (d) Cametti, M.; Nissinen, M.; Dalla Cort, A.; Mandolini, L.; Rissanen, K. *Chem. Commun.* **2003**, 2420. (e) Cametti, M.; Nissinen, M.; Dalla Cort, A.; Mandolini, L.; Rissanen, K. *J. Am. Chem. Soc.* **2005**, *127*, 3831.

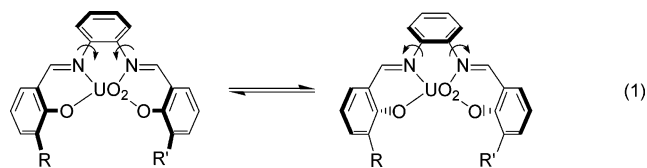
(9) For theoretical work, see: Brynda, M.; Wesolowski, T. A.; Wojciechowski, K. *J. Phys. Chem. A* **2004**, *108*, 5091.

(10) Dalla Cort, A.; Mandolini, L.; Palmieri, G.; Pasquini, C.; Schiaffino, L. *Chem. Commun.* **2003**, 2178.

(11) Dalla Cort, A.; Mandolini, L.; Pasquini, C.; Schiaffino, L. *Org. Lett.* **2004**, *6*, 1697.



Chirality in nonsymmetrical uranyl salophen complexes represents a peculiar case in the chemistry of metal coordination complexes.¹² In unhindered complexes (eq 1), the metal ion does not act as a stereogenic center in a strict sense but because of its large ionic radius dissymmetrizes the entire structure creating a curvature.¹³ On the other hand, the very presence of bulky substituents such as those in **1–4** would presumably cause the ligand itself to exist as detectable chiral atropisomers.¹⁴ It was felt therefore that an analysis of the stereomutations of the free ligands and of the stereodynamic effects of substituents is not only interesting per se, but would also provide valuable insights into the problem of how the conformational mobility of the ligands is affected upon coordination to the uranyl dication.



Here, we report the results of an extensive conformational investigation of ligands **1–4**. The study was carried out by dynamic ¹H NMR spectroscopy (DNMR) supported by ab initio and molecular mechanics calculations, in combination with dynamic HPLC (DHPLC) on enantioselective columns.

Results and Discussion

Free salophen ligands **1–4** were easily obtained from the corresponding uranyl complexes^{10,11} on elution with a dichloromethane/acetone mixture (75/25 v/v) through a plug of silica gel. Under such conditions, complexes

(12) (a) von Zelewsky, A. *Stereochemistry of Coordination Compounds*; Wiley: Chichester, 1996. (b) Knof, U.; von Zelewsky, A. *Angew. Chem.* **1999**, *111*, 312; *Angew. Chem., Int. Ed.* **1999**, *38*, 302.

(13) Dalla Cort, A.; Mandolini, L.; Pasquini, C.; Schiaffino, L. *New J. Chem.* **2004**, *28*, 1198.

(14) Eliel, E. L.; Wilen, S. K. *Stereochemistry of Organic Compounds*; Wiley: New York, 1994; p 550.

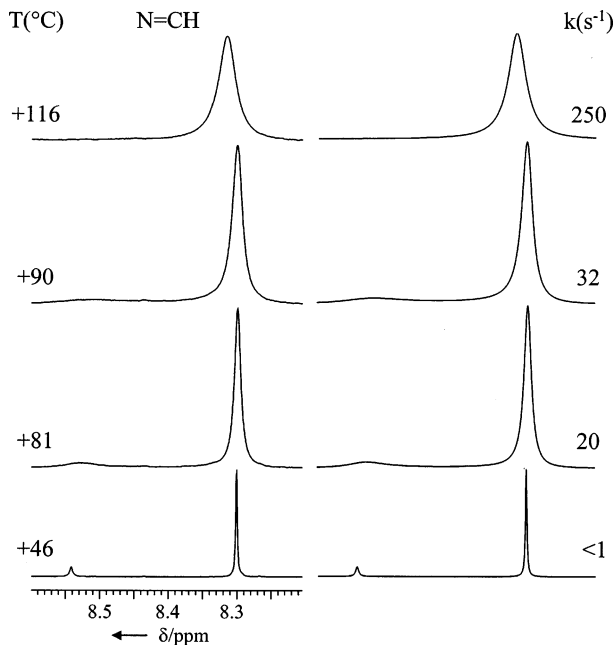


FIGURE 1. Temperature dependence of the ^1H NMR signal (600 MHz) of the N=CH hydrogen of **2** in $\text{DMSO-}d_6$ (left) and the spectral simulation based on the given rate constants (right).

readily dissociated and the neutral ligands were recovered in virtually quantitative yields as yellow solids.

The low-field singlets (δ 15–13) in the ^1H NMR spectra of all of the ligands indicate that the phenolic hydroxyls are strongly hydrogen bonded to the imine nitrogens, as shown in Scheme 1. These hydrogen bonds stabilize the imine bonds in an *E* configuration.

The ^1H NMR spectrum (600 MHz) of **2** in $\text{DMSO-}d_6$ displays two groups of signals, due to a pair of conformers with different populations. This is particularly evident in the case of the N=CH hydrogen, which exhibits two single lines separated by 144 Hz with a 15:85 intensity ratio (Figure 1). In addition, the geminal methyl groups of the isopropyl substituent appear diastereotopic in that a pair of doublet signals for both the major and minor conformer is displayed (Figure 2). The observed diastereotopicity implies that both conformers do not possess a plane of symmetry and, as a consequence, also comprise a pair of enantiomers. In a low polarity solvent such as C_6D_6 only the spectrum corresponding to the major of the two conformers is observed. The observed decrease in stability of the minor component on going from the polar $\text{DMSO-}d_6$ to the apolar C_6D_6 is taken as an indication of a larger dipole moment of the minor conformer compared to its major companion.

The presence of a pair of conformers can be explained by the existence of two stereogenic axes ($a_{1,8}$ and $a_{6,7}$ aligned to the C1–N8 and C6–N7 bonds, respectively) that are conceivably due to the restricted rotation about the two Ar–N bonds. Inspection of molecular models suggests that the planes containing the C=N moieties are significantly twisted with respect to that of the *o*-phenylenediamine moiety, owing to rather large steric effects. Such a situation implies that the two imine carbon atoms can adopt either a *cis* or a *trans* disposition with respect to the plane of the *o*-phenylenediamine ring

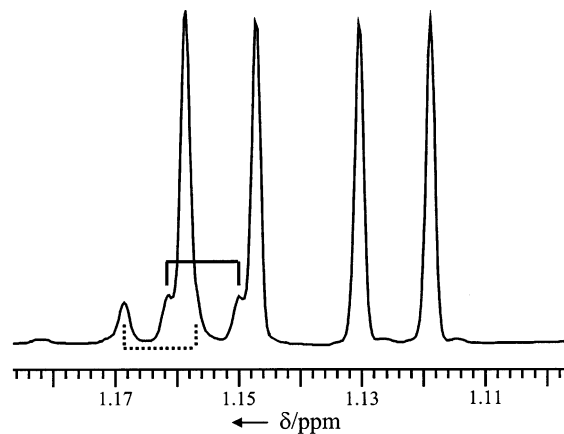


FIGURE 2. ^1H NMR (600 MHz) spectral region of the methyl groups of **2** in $\text{DMSO-}d_6$ at ambient temperature displaying two doublets ($J = 6.9$ Hz, $\Delta\nu = 17.0$ Hz) for the major diastereoisomer (85%). One of the four lines of the minor form ($J = 6.9$ Hz, $\Delta\nu = 4.4$ Hz) is hidden by the low-field line of its major companion.

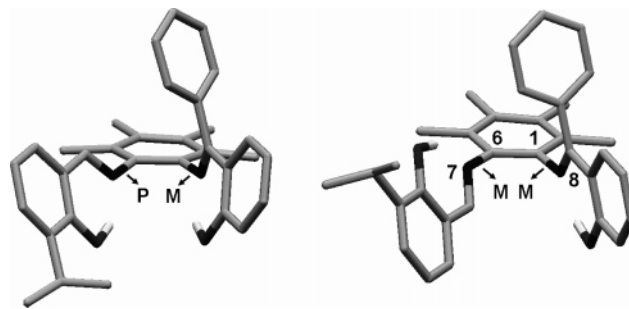


FIGURE 3. Ab initio computed structures of the *cis* and *trans* conformers of compound **2**. The hydrogen atoms, except those of the hydroxyls, are omitted for clarity.

(Figure 3), consistent with the detection of two conformers in DMSO solution. Both conformers are asymmetric, thus accounting for the observed diastereotopicity of the geminal methyl groups of the isopropyl moiety. Such an asymmetry implies the existence of two enantiomeric forms per each conformer. The relative configurations of the two stereogenic axes in the *cis* and *trans* forms are $[a_{1,8}\text{P}(\text{M}); a_{6,7}\text{M}(\text{P})]$ and $[a_{1,8}\text{P}(\text{M}); a_{6,7}\text{P}(\text{M})]$, respectively.

Ab initio calculations¹⁵ indicate that such asymmetric *cis* and *trans* structures (Figure 3) correspond indeed to energy minima since the vibrational frequency analysis shows the absence of imaginary frequencies in both cases.

(15) HF/6-31G(d) level: Gaussian 03, Revision C.02. Frisch, M. J.; Trucks, G. W.; Schlegel, H. B.; Scuseria, G. E.; Robb, M. A.; Cheeseman, J. R.; Montgomery, J. A., Jr.; Vreven, T.; Kudin, K. N.; Burant, J. C.; Millam, J. M.; Iyengar, S. S.; Tomasi, J.; Barone, V.; Mennucci, B.; Cossi, M.; Scalmani, G.; Rega, N.; Petersson, G. A.; Nakatsuji, H.; Hada, M.; Ehara, M.; Toyota, K.; Fukuda, R.; Hasegawa, J.; Ishida, M.; Nakajima, T.; Honda, Y.; Kitao, O.; Nakai, H.; Klene, M.; Li, X.; Knox, J. E.; Hratchian, H. P.; Cross, J. B.; Bakken, V.; Adamo, C.; Jaramillo, J.; Gomperts, R.; Stratmann, R. E.; Yazyev, O.; Austin, A. J.; Cammi, R.; Pomelli, C.; Ochterski, J. W.; Ayala, P. Y.; Morokuma, K.; Voth, G. A.; Salvador, P.; Dannenberg, J. J.; Zakrzewski, V. G.; Dapprich, S.; Daniels, A. D.; Strain, M. C.; Farkas, O.; Malick, D. K.; Rabuck, A. D.; Raghavachari, K.; Foresman, J. B.; Ortiz, J. V.; Cui, Q.; Baboul, A. G.; Clifford, S.; Cioslowski, J.; Stefanov, B. B.; Liu, G.; Liashenko, A.; Piskorz, P.; Komaromi, I.; Martin, R. L.; Fox, D. J.; Keith, T.; Al-Laham, M. A.; Peng, C. Y.; Nanayakkara, A.; Challacombe, M.; Gill, P. M. W.; Johnson, B.; Chen, W.; Wong, M. W.; Gonzalez, C.; Pople, J. A. Gaussian, Inc., Wallingford, CT, 2004.

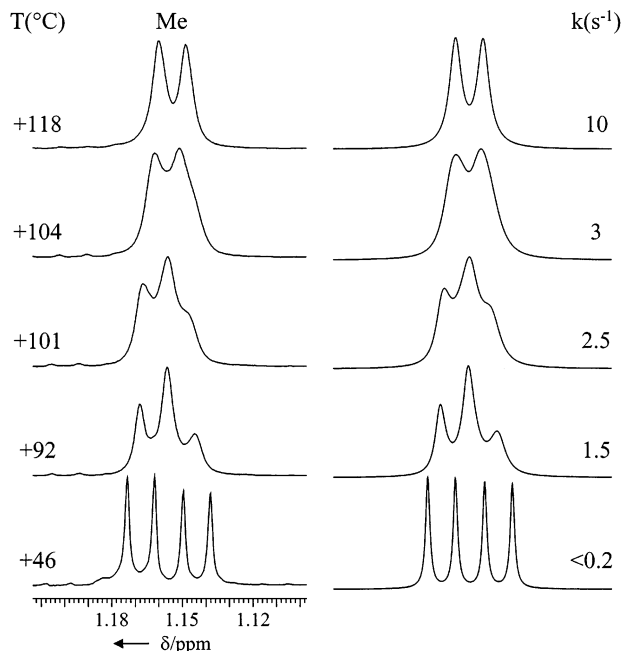


FIGURE 4. Temperature dependence of the ^1H NMR signals (600 MHz) of the geminal methyls of the isopropyl group of **2** in $\text{DMSO-}d_6$ (left) and the spectral simulation based on the given rate constants (right).

The *cis* form is computed to be less stable than its *trans* form by $3.2 \text{ kcal mol}^{-1}$. Such a large energy difference suggests that in the isolated molecule the equilibrium would be completely shifted toward the latter, a result in agreement with the observation of a single conformer in C_6D_6 solution. The presence of a second conformer in $\text{DMSO-}d_6$ can be explained by the fact that the dipole moment of the *cis* form (6.4 D) is computed to be larger than that of the *trans* form (2.5 D). The form with a larger dipole moment is thus significantly stabilized, and its presence becomes detectable in the polar $\text{DMSO-}d_6$.

Molecular Mechanics calculations (MMFF force field)¹⁶ confirm the existence of two energy minima corresponding to a *cis* and a *trans* form. When a dielectric constant equal to that of benzene ($\epsilon = 3$)¹⁷ is used, the energy of the *cis* form was computed to be $2.6 \text{ kcal mol}^{-1}$ higher than that of the *trans* form, whereas for a dielectric constant equal to that of DMSO ($\epsilon = 47$)¹⁷ the difference decreased to $1.4 \text{ kcal mol}^{-1}$. The ratio of the two conformers at ambient temperature is thus predicted to be 99:1 and 91:9 in benzene and DMSO, respectively, in substantial agreement with the experimental observations.

On increasing the temperature of the DMSO solution, the two lines of the $\text{N}=\text{CH}$ hydrogen broaden and eventually coalesce into a single signal above $+100 \text{ }^\circ\text{C}$ (Figure 1), the process being fully reversible. A similar behavior is exhibited by the doublet signals of the geminal methyl groups that coalesce, yielding a single doublet (Figure 4).

Line shape simulation¹⁸ of the $\text{N}=\text{CH}$ signals of the spectrum in $\text{DMSO-}d_6$ provided the rate constants at various temperatures for the *trans* to *cis* interconversion (Figure 1) along with a value of $18.8 \pm 0.2 \text{ kcal mol}^{-1}$ for the corresponding free energy of activation. Simulation of the lines of the geminal methyl signals (Figure 4) yielded in a similar way the free energy of activation for the interconversion of the enantiomers, $\Delta G^\ddagger = 21.4 \pm 0.4 \text{ kcal mol}^{-1}$. It appears therefore that the barrier for the *trans* to *cis* interconversion is lower than that needed for the enantiomerization process. Since there are two aryl substituents bonded to C10, and only one to C9, it seems likely that rotation about the C6–N7 bond is less hindered than rotation about the C1–N8 bond. Consequently, the *trans* to *cis* interconversion can be conceivably attributed to the rotation about the C6–N7 bond, whereas the rotation about the C1–N8 bond is the slow step of the slower enantiomerization.

In the analogous compound **1** that lacks the four methyl substituents, the *cis* and *trans* forms were not observed in DMSO solution, and in addition, the methyl groups of the isopropyl moiety appear enantiotopic (isochronous) even at $-150 \text{ }^\circ\text{C}$ in CHF_2Cl solution. This is a clear indication that the features observed in the spectra of **2** are due to the restricted rotations caused by the hindrance exerted by the methyl groups bonded to C2 and C5.

When the *cis* and *trans* conformers of **2** are averaged by the rapid C6–N7 rotation the two residual enantiomers ($a_{1,8}\text{P}$) and ($a_{1,8}\text{M}$) are still present since they must overcome a higher barrier to interconvert into each other. Since a barrier of $21.4 \text{ kcal mol}^{-1}$ corresponds to a half-life on the order of 5 h at $0 \text{ }^\circ\text{C}$, a physical separation of the enantiomers is feasible at the given temperature. Such a separation was actually achieved. As shown in Figure 5, two chromatographic peaks, corresponding to the two enantiomers, appear with equal (trace a) or opposite phase (trace b) when UV or CD detectors are employed, respectively.

When the enantioselective column was warmed above ambient temperature a change of the chromatogram shapes took place and a single average peak was eventually observed above $+50 \text{ }^\circ\text{C}$ (Figure 6, left). Computer line shape simulation (Figure 6, right) yielded the rate constants for the enantiomerization process, along with a ΔG^\ddagger value (Table 1) which compares well with that determined by DNMR.

In the HPLC experiment, the presence of the *cis* form was never detected. This agrees with the observation that only a solvent with a very high dielectric constant, such as DMSO, allows the *cis* conformer to be sufficiently populated at equilibrium. Thus, a physical separation of the *cis* from the *trans* form could not be attempted since DMSO cannot be used in the HPLC experiment.

As observed for **2**, the ^1H spectrum (600 MHz) of **3** in $\text{DMSO-}d_6$ shows the presence of two conformers in a similar proportion (17:83). On raising the temperature, the corresponding signals broaden and eventually merge into averaged signals above $+110 \text{ }^\circ\text{C}$, the process being fully reversible. Line shape simulation provided an activation barrier for the inversion of the stereogenic $a_{6,7}$ which is equal to that measured for the corresponding

(16) Conformational searches were carried out by Macromodel version 7.2 (Columbia University, NY) using the following options: MMFFs 94 Force Field, Monte Carlo stochastic algorithm with 3000 generated structures, minimization by PR conjugate gradient. All the rotatable bonds were explored.

(17) Landolt-Börnstein, Band II, Teil 6, Springer-Verlag: Berlin, 1959.

(18) QCPE program no. 633, Indiana University, Bloomington, IN.

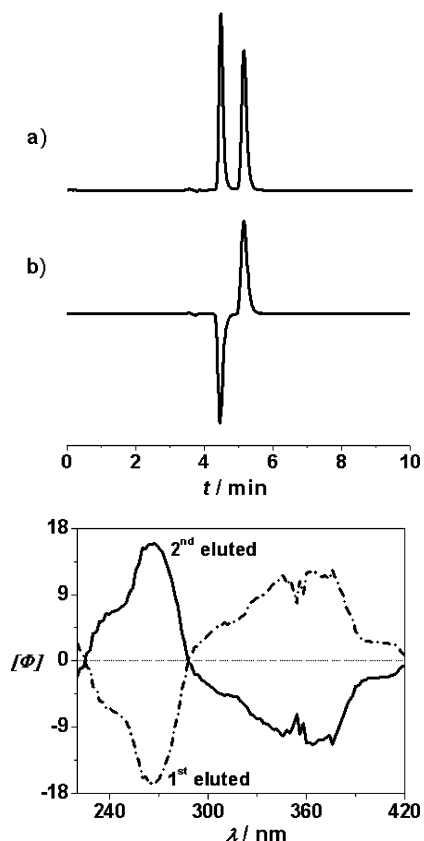


FIGURE 5. Top: HPLC resolution of the enantiomers of **2** at 0 °C on a Chiralcel-OD column (eluent: *n*-hexane/2-propanol/methanol 95/3.5/1.5, flow rate 1 mL/min) with UV (trace a) and CD (trace b) detection at 254 nm. Bottom: CD spectra of the enantiomers taken at 0 °C.

process in **2** (Table 1). The spectrum in C_6D_6 confirms that only the major conformer is present in an apolar solvent.

Because of the absence of the isopropyl group, no NMR evidence could be obtained for the molecular asymmetry responsible for the existence of a pair of enantiomers. However, the 1H spectrum taken in a chiral environment, obtained by addition of an enantiomerically pure Pirkle's alcohol¹⁹ to a C_6D_6 solution of **3** shows that a number of lines, e.g., those of the imine proton and of a methyl group, were split into 1:1 pairs (Figure 7).

The two enantiomers were separated on an enantioselective HPLC column. The enantiomerization barrier, as determined by DHPLC (Supporting Information), was found to have a value almost equal to that observed for compound **2** (Table 1).

The naproxen moiety of compound **4** comprises an enantiopure chiral center in the *S* configuration. For this reason, two diastereoisomeric pairs are expected to occur, instead of the two enantiomeric pairs of the previous cases. Consistently, in a DMSO solution many 1H signals of the major *trans* conformer are split into two signals of slightly different intensity (52:48). The complexity of the proton spectral lines prevented an analogous observation for the *cis* conformer, even at 600 MHz. Nevertheless,

(19) We used *R*-1-(9-anthryl)-2,2,2-trifluoroethanol as chiral solvating agent. See: Pirkle, W. H.; Sikkenga, D. L.; Pavlin, M. S. *J. Org. Chem.* **1977**, *42*, 384.

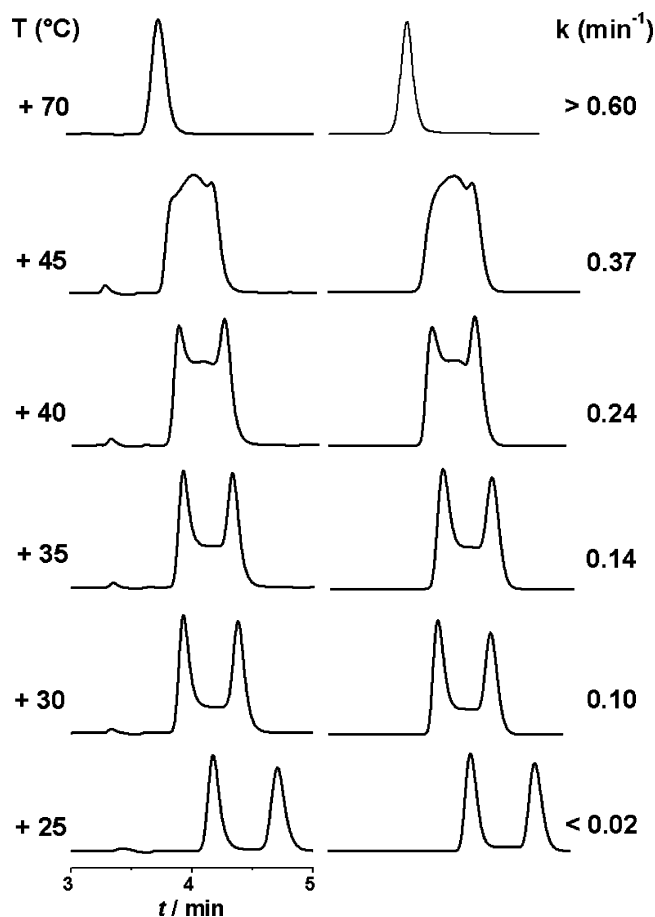


FIGURE 6. Temperature-dependent chromatographic profiles of **2** on Chiralcel-OD column. Left: experimental chromatogram (eluent: *n*-hexane/2-propanol/methanol 95/3.5/1.5, flow rate 1 mL/min, UV detection at 254 nm) as function of temperature. Right: computer simulation profiles obtained with the given rate constants for the on-column enantiomerization process.

the ^{13}C spectrum showed that many lines of both conformers are doublets of nearly equal intensity.

Line shape simulation of the NMR spectrum in DMSO- d_6 above ambient temperature provided a value of 19.3 ± 0.2 kcal mol⁻¹ for the barrier of the *trans* to *cis* interconversion, which is very similar to the values of the corresponding barriers in **2** and **3** (Table 1). In the present case, the signals exchange of resonances attributable to diastereomerization was unfortunately obscured by the *trans* to *cis* isomerization. This problem was circumvented by replacement of the polar DMSO- d_6 with the less polar, high boiling nitrobenzene- d_5 . Since in the latter solvent only the *trans* form was present in detectable amounts, any interference from the *trans* to *cis* interconversion was avoided. Line shape simulation (Supporting Information) gave a value of 21.9 kcal mol⁻¹ for the barrier of the mutual exchange between the ($\alpha_{1,8}P$;S) and ($\alpha_{1,8}M$;S) diastereoisomers. Not surprisingly, such a value is virtually identical to the values found for the enantiomerization process in **2** and **3**.

For the sake of uniformity, compound **4** was subjected to DHPLC analysis under the same conditions used for compounds **2** and **3**. At +10 °C, the two diastereoisomers of the *trans* form appeared as two well resolved peaks

TABLE 1. Interconversion Barriers (ΔG^\ddagger in kcal mol⁻¹, Errors in Parentheses) Measured for Compounds 2–4 from DNMR and DHPLC Experiments

configuration inversion	2	3	4
about $a_{6,7}^a$	18.8 (0.2), DNMR	18.8 (0.2), DNMR	19.3 (0.2), DNMR
about $a_{1,8}^b$	21.4 (0.4), DNMR	21.9 (0.2), DHPLC	21.9 (0.2), DNMR
	21.8 (0.2), DHPLC		21.9 (0.2), DHPLC

^a Corresponding to *trans* to *cis* interconversion. ^b Corresponding to enantiomerization in 2 and 3, and to diastereomerization in 4.

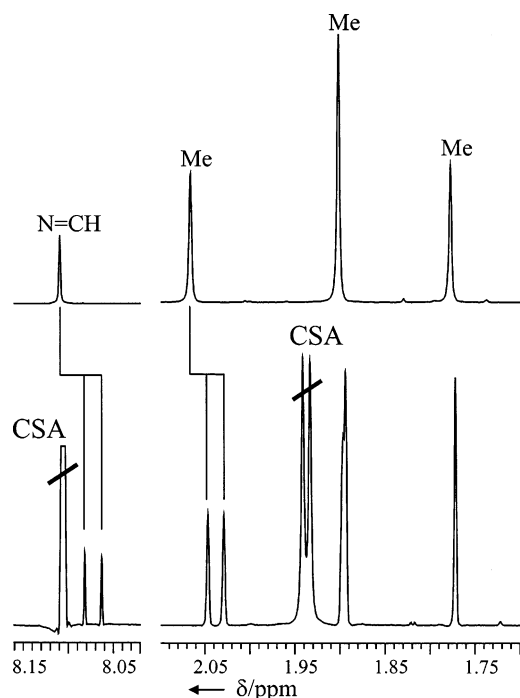


FIGURE 7. Portions of the 600 MHz spectrum of 3 in C₆D₆ (top). The same region after addition of a chiral solvating agent (CSA) showing the splitting due to the presence of the two enantiomers (bottom).

(Supporting Information), with an intensity ratio of 54:46, very close to that measured by NMR. Analysis of the temperature-dependent chromatographic profiles afforded an interconversion barrier equal to that determined by DNMR (Table 1).

Conclusions

In conclusion, the complex stereomutations occurring in sterically hindered salophen ligands 2–4 have been analyzed in terms of restricted rotations about the C1–N8 and C6–N7 single bonds, whose energy barriers have been accurately determined by means of DNMR and DHPLC techniques. The results provide an additional illustration not only of the equivalence of the two techniques, whenever applicable, but also of their complementarity.²⁰

Comparison of the height of the barrier for diastereomerization in 4 (21.9 kcal mol⁻¹) with that for diastereomerization in the corresponding uranyl complex (24.6 kcal mol⁻¹),¹¹ shows that coordination to the metal center decreases significantly, albeit not dramatically, the stereochemical lability of the ligand.

Experimental Section

Materials. Uranyl complexes of ligands 1, 2,¹⁰ and 4¹¹ were available from previous investigations.

[[3,4,5,6-Tetramethyl-1-phenylene[E-nitrilomethylidyne]phenyl(2-hydroxyphenyl)]-2-phenylene[nitrilomethylidyne(2-hydroxy-3-phenylphenyl)](2H-N,N',O,O')-dioxouranium (3-2H·UO₂). This compound was prepared in 72% yield according to a previously reported procedure.²¹ ¹H NMR (600 MHz, acetone-*d*₆, 25 °C): δ 1.88 (s, 3H, Me); 1.94 (s, 3H, Me); 2.22 (s, 3H, Me); 2.50 (s, 3H, Me); 6.38–6.40 (t, 1H, CH, J = 7.8 Hz); 6.80–6.77 (t, 1H, CH, J = 7.3 Hz); 6.98–6.99 (d, 1H, CH, J = 9.0 Hz); 7.02–7.03 (dd, 1H, CH, J = 7.9, 1.5 Hz); 7.19–7.22 (t, 1H, CH, J = 7.3 Hz); 7.27–7.28 (bd, 1H, CH, J = 7.32 Hz); 7.39–7.41 (t, 1H, CH, J = 7.6 Hz); 7.44–7.47 (m, 2H); 7.50–7.52 (t, 2H, J = 7.9 Hz); 7.55–7.57 (t, 1H, CH, J = 7.6 Hz); 7.63–7.65 (dd, 1H, CH, J = 7.3, 1.8 Hz); 7.68–7.69 (bd, 1H, CH, J = 7.3 Hz); 7.77–7.79 (dd, 1H, CH, J = 7.94, 1.83 Hz); 7.84–7.85 (bd, 2H, J = 7.02 Hz); 9.66 (s, 1H, CH=N). ¹³C NMR (75 MHz, acetone-*d*₆, 25 °C): δ 17.0 (Me); 17.1 (Me); 17.6 (Me); 18.6 (Me); 116.9 (CH); 118.1 (CH); 121.8 (CH); 125.5 (CH); 125.5 (CH); 125.6 (CH); 125.8 (CH); 127.6 (CH); 128.7 (Cq); 128.8 (Cq); 129.0 (2CH); 130.9 (CH); 131.3 (2CH); 131.7 (Cq); 133.6 (CH); 133.7 (CH); 134.6 (CH); 135.6 (CH); 135.6 (CH); 135.7 (CH); 135.0 (CH); 137.1 (CH); 139.9 (CH); 141.3 (Cq); 145.3 (Cq); 145.4 (Cq); 168.3 (Cq); 169.4 (Cq); 173.4 (Cq); 175.3 (CH). MS-ESI-TOF for C₃₆H₃₀N₂O₄U: calcd 792.27, found 792.0 ([M]⁻), 811.0 ([MF]⁻). Anal. Calcd for C₃₆H₃₀N₂O₄U·3H₂O: C, 51.07; H, 4.29; N, 3.31. Found: C, 51.42; H, 4.00; N, 3.20.

2-[(E)-{(2-[(1E)-(2-hydroxyphenyl)(phenyl)methylene]amino}phenyl)imino]methyl]-6-isopropylphenol (1). The following procedure is typical. The uranyl complex of 1 (0.200 g, 0.285 mmol) was dissolved in a dichloromethane/acetone mixture (75/25 v/v), and the resulting solution was eluted through a plug of silica gel. The title compound (0.127 g, 0.278 mmol) was obtained as a yellow solid. Mp: 120–123 °C. ¹H NMR (600 MHz, CDCl₃, 25 °C): δ 1.18 (d, 3H, Me, J = 7.1 Hz); 3.34 (septet, 1H, CH, J = 7.1 Hz); 6.71 (ddd, 1H, CH, J = 8.6, 7.3, 1.2 Hz); 6.80 (m, 1H, CH); 6.87 (t, 1H, CH, J = 7.5 Hz); 7.00 (m, 1H); 7.04–7.10 (m, 6H, 6CH); 7.15 (dd, 1H, CH, J = 7.7, 1.6 Hz); 7.20 (m, 2H); 7.26 (m, 1H, CH); 7.29 (dd, 1H, CH, J = 7.5, 1.6); 7.36 (ddd, 1H, CH, J = 8.6, 7.3, 1.7 Hz); 8.35 (s, 1H, CH=N); 13.18 (s, 1H, OH); 14.12 (bs, 1H, OH). ¹³C NMR (150.81 MHz, CDCl₃, 25 °C): δ 22.3 (Me); 26.4 (CH); 117.8 (CH); 118.0 (CH); 118.6 (CH); 118.7 (CH); 119.0 (CH); 119.6 (Cq); 123.1 (CH); 125.5 (CH); 126.6 (CH); 127.9 (2CH); 128.5 (2CH); 128.9 (CH); 129.8 (CH); 129.9 (CH); 132.3 (CH); 133.4 (CH); 134.6 (Cq); 136.7 (Cq); 140.4 (Cq); 141.5 (Cq); 158.8 (Cq); 162.7 (Cq); 163.4 (CH=N); 174.6 (Cq=N). MS ESI TOF for C₂₉H₂₆N₂O₂ Na⁺: calcd 457.1883, found 457.1892. Anal. Calcd for C₂₉H₂₆N₂O₂: C, 80.16; H, 6.03; N, 6.45. Found: C, 79.83; H, 6.47; N, 6.05.

2-[(E)-{(2-[(1E)-(2-hydroxyphenyl)(phenyl)methylene]amino}-3,4,5,6-tetramethylphenyl)imino]methyl]-6-isopropylphenol (2). This compound was obtained as above from the corresponding uranyl complex as a yellow solid. Mp: 166–168 °C. ¹H NMR (600 MHz, C₆D₆, 25 °C): δ 1.21 (d, 3H, Me, J = 7.1 Hz); 1.23 (d, 3H, Me, J = 7.0 Hz); 1.80 (s, 3H, Me); 1.91 (s, 3H, Me); 1.92 (s, 3H, Me); 2.08 (s, 3H, Me); 3.60 (septet,

(20) Gasparrini, F.; Grilli, S.; Leardini, R.; Lunazzi, L.; Mazzanti, A.; Nanni, D.; Pierini, M.; Pinamonti, M. *J. Org. Chem.* **2002**, *67*, 3089.

(21) Dalla Cort, A.; Pasquini, C.; Miranda Murua, J. I.; Pons, M.; Schiaffino, L. *Chem. Eur. J.* **2004**, *10*, 3301.

1H, $J = 7.0$ Hz); 6.31 (ddd, 1H, CH, $J = 7.2, 7.0, 1.1$ Hz); 6.65 (t, 1H, CH, $J = 7.1$ Hz); 6.82 (tt, 1H, CH, $J = 7.4, 1.3$ Hz); 6.90–6.97 (m, 4H, CH); 7.00 (dd, 1H, $J = 7.6, 1.6$ Hz); 7.04 (bd, 2H, CH); 7.06 (dd, 1H, CH, $J = 7.7, 1.3$ Hz); 7.19 (d, 1H, CH, $J = 8.4$ Hz); 8.08 (s, 1H, CH=N); 13.78 (s, 1H, OH); 14.69 (bs, 1H, OH). ^{13}C NMR (150.81 MHz, C_6D_6 , 25 °C): δ 15.3 (Me); 16.0 (Me); 16.1 (Me); 16.3 (Me); 22.4 (Me-*ipr*); 22.5 (Me-*ipr*); 27.1 (CH-*ipr*); 118.2 (CH); 118.3 (CH); 118.8 (Cq); 119.0 (CH); 119.9 (Cq); 125.2 (Cq); 126.4 (Cq); 127.6 (CH); 128.1 (CH); 129.2 (CH); 130.0 (CH); 130.2 (CH); 131.9 (Cq); 132.3 (Cq); 132.5 (CH); 133.4 (CH); 135.7 (Cq); 135.8 (Cq); 136.5 (Cq); 136.7 (Cq); 159.2 (Cq); 163.6 (Cq); 168.5 (CH=N); 174.5 (Cq=N). MS ESI TOF for $\text{C}_{33}\text{H}_{35}\text{N}_2\text{O}_2^+$: calcd 491.2699, found 491.2716. Anal. Calcd for $\text{C}_{33}\text{H}_{34}\text{N}_2\text{O}_2$: C, 80.78; H, 6.98; N, 5.71. Found: C, 80.54; H, 7.58; N, 5.57.

2-[(E)-(2-[(1E)-(2-hydroxyphenyl)(phenyl)methylene]amino)-3,4,5,6-tetramethylphenyl]imino]methyl]-6-phenylphenol (3). This compound was obtained as above from the corresponding uranyl complex as a yellow solid. Mp: 110–112 °C. ^1H NMR (600 MHz, C_6D_6 , 25 °C): δ 1.79 (s, 3H, Me); 1.92 (s, 6H, 2Me); 2.08 (s, 3H, Me); 6.34 (ddd, 1H, CH, $J = 7.4, 7.3, 1.2$ Hz); 6.64 (t, 1H, CH, $J = 7.6$ Hz); 6.75 (tt, 1H, CH, $J = 7.5, 1.2$ Hz); 6.85 (t, 2H, $J = 7.6$ Hz); 6.91 (dd, 1H, $J = 7.7, 1.5$ Hz); 6.96–7.02 (m, 3H, CH); 7.07 (dd, 1H, $J = 7.7, 1.5$ Hz); 7.15 (m, 1H, CH, benzene overlapped); 7.21 (m, 2H, CH); 7.27 (t, 2H, 2CH, $J = 7.7$ Hz); 7.68 (m, 2H, 2CH); 8.12 (s, 1H, CH=N); 14.00 (s, 1H, OH); 14.70 (bs, 1H, OH). ^{13}C NMR (150.81 MHz, C_6D_6 , 25 °C): δ 15.3 (Me); 16.0 (Me); 16.1 (Me); 16.3 (Me); 118.3 (2CH); 119.3 (CH); 119.4 (Cq); 119.6 (Cq); 119.9 (Cq); 125.2 (Cq); 126.6 (Cq); 127.2 (CH); 127.3 (2CH); 128.1 (2CH); 128.2 (2CH); 129.3 (CH); 129.9 (2CH); 130.3 (Cq); 132.0 (CH) 132.5 (Cq); 132.7 (CH); 133.6 (CH); 134.3 (CH) 135.6 (Cq); 135.8 (Cq); 136.4 (Cq); 138.3 (Cq); 159.0 (Cq); 163.6 (Cq); 168.3 (CH=N); 174.7 (Cq=N). MS ESI TOF for $\text{C}_{36}\text{H}_{33}\text{N}_2\text{O}_2^+$: calcd 525.2542, found 525.2531. Anal. Calcd for $\text{C}_{36}\text{H}_{32}\text{N}_2\text{O}_2\cdot\text{CH}_3\text{OH}$: C, 79.83; H, 6.52; N, 5.03. Found: C, 80.57; H, 6.30; N, 5.13.

2-Hydroxy-3-[(E)-(2-[(1E)-(2-hydroxyphenyl)(phenyl)methylene]amino)-3,4,5,6-tetramethylphenyl]imino]methyl]phenyl-(2S)-2-(6-methoxy-2-naphthyl)propanoate (4). This compound was obtained as above from the corresponding uranyl complex as a yellow solid. Mp: 156–158 °C. ^1H NMR (600 MHz, C_6D_6 , 25 °C): δ 1.67 and 1.70 (d, 3H, Me, $J = 7.0$ Hz); 1.70 (s, 3H, Me); 1.79 and 1.81 (s, 3H, Me); 1.92 and 1.93 (s, 3H, Me) 2.09 and 2.11 (s, 3H, Me); 3.38 (s, 3H, OMe); 4.10 (m, 1H, CH-Me); 6.32 (m, 1H, CH); 6.74 (m, 1H, CH); 6.80–6.92 (m, 2H, CH); 6.93–7.02 (m, 7H); 7.19 (m, 2H); 7.53 (t, 1H, CH, $J = 9.6$ Hz); 7.59–7.66 (m, 2H); 7.76 (d, 1H, CH, $J = 6.6$); 7.94 and 7.945 (s, 1H, CH=N); 13.76 (s, 1H, OH); 14.68 (bs, 1H, OH). ^{13}C NMR (150.81 MHz, C_6D_6 , 25 °C): δ 15.31 and 15.33 (Me); 16.96 (Me); 16.07 and 16.30 (Me); 19.11 and 19.28 (Me), 45.74 and 45.79 (CH), 54.77 (OMe); 105.33 (CH); 118.20 (CH); 118.35 (CH); 118.51 (CH); 119.34 (CH); 119.78 (CH); 120.43 (Cq); 125.60 (Cq); 125.77 (Cq); 126.12 (Cq); 126.28 (CH); 126.67 (CH); 126.92 (CH); 127.50 (CH); 128.19 (CH); 128.56 (CH); 128.69 (CH); 129.30 (Cq); 129.34 (CH); 129.41 (CH); 129.65 (Cq); 129.82 (Cq); 129.85 (CH); 131.91 (Cq); 132.57 (Cq); 132.70 (CH); 133.57 (CH); 134.42 (Cq); 135.52 (Cq); 135.64 (Cq); 135.81 (Cq); 136.04 (Cq); 136.17 (Cq); 139.79 (Cq); 139.84 (Cq); 153.80 (Cq); 158.22 (Cq); 163.52 (Cq); 167.57 and 167.68 (CH=N); 171.99 (Cq=N); 172.19 (Cq=N); 174.64 (CO). MS ESI TOF for $\text{C}_{44}\text{H}_{40}\text{N}_2\text{O}_5\text{Na}^+$: calcd 699.2835, found 699.2863. Anal. Calcd for $\text{C}_{44}\text{H}_{40}\text{N}_2\text{O}_5$: C, 78.08; H, 5.96; N, 4.14. Found: C, 78.51; H, 6.40; N, 3.99.

NMR Measurements. NMR spectra were recorded at 300, 400, or 600 MHz for ^1H and 75.4, 100.6, or 150.8 MHz for ^{13}C . The assignments of the ^{13}C signals were obtained by DEPT and 2D experiments (gHSQC sequence). The samples for the NMR low-temperature measurements were prepared by connecting to a vacuum line the NMR tubes containing the compound and some C_6D_6 for locking purpose and condensing

therein the gaseous CHF_2Cl under cooling with liquid nitrogen. The tubes were subsequently sealed in vacuo and introduced into the precooled probe of the spectrometer. The temperatures were calibrated by substituting the sample with a precision Cu/Ni thermocouple before the measurements. Complete fitting of dynamic NMR line shapes was carried out using a PC version of the DNMR-6 program.¹⁸ At least five different temperature spectra were used for the simulations.

Chromatography. Analytical liquid chromatography was performed on a HPLC system equipped with a Rheodyne model 7725i 20 μL loop injector, a Waters Mod 600 pump, a Thermo Finnigan photodiode array Mod UV6000LP detector, and a JASCO Mod 995 CD detector. Chromatographic data were collected and processed using Chromquest software (Waters, Milford, MA). Chiralcel-OD (cellulose tris(3,5-dimethyl phenylcarbamate) coated on a 5 μm macroporous silica gel) column (250 \times 4.6 mm, L \times i.d.) was obtained from Chiral Technologies. Variable-temperature chromatography with UV and CD detection was performed by placing the column inside a thermally insulated container cooled by the expansion of liquid carbon dioxide. The flow of liquid CO_2 and the column temperature were regulated by a solenoid valve, a thermocouple and an electric controller. Temperature variations after thermal equilibration were within ± 0.1 °C.

Simulation of Dynamic Chromatograms. Simulation of variable-temperature experimental chromatograms were performed by use of the dedicate made home computer program Auto DHPLC y2k (Auto Dynamic HPLC), which implements both stochastic and theoretical plates models²² and the possibility to taking into account tailing effects. Both chromatographic and kinetic parameters can be automatically optimized by simplex algorithm until the best agreement between experimental and simulated dynamic chromatograms is obtained. All the simulations in this paper were performed employing the stochastic model, taking into account tailing effects.

Computations. A complete conformational search, using Molecular Mechanics (MMFF Force Field),¹⁶ was performed to locate the global minima of the two conformations of **2**. Ab initio computations were carried out on these structures at the HF/6-31G(d) level by means of the Gaussian 03 series of programs¹⁵ (the standard Berny algorithm in redundant internal and default criteria of convergence were employed). Harmonic vibrational frequencies were calculated in order to ascertain the nature of all the stationary points. For each optimized ground state the frequency analysis showed the absence of imaginary frequencies. The corresponding optimized structures are reported in the Supporting Information.

Acknowledgment. Financial support from MIUR, COFIN 2003, Progetto Dispositivi Supramolecolari was received by L.M., A.D.C., C.P., and L.S. Financial support from MIUR-COFIN 2003 039537 Ingegneria di Sistemi di Separazione ad Elevate Prestazioni, Sensori e Arrays Basati sul Riconoscimento Molecolare Chemo- e Stereoselettivo was received by F.G., M.P., and R.R. Financial support from the University of Bologna (Funds for selected research topics and RFO) and from MIUR-COFIN 2003, Rome (national project “Stereoselection in Organic Synthesis”) was received by L.L. and A.M.

Supporting Information Available: Computational details, temperature-dependent chromatographic profiles, and HPLC resolution of the enantiomers of **3** and of the diastereoisomers of **4**, and temperature dependence of the ^1H signals (600 MHz) of **4**. This material is available free of charge via the Internet at <http://pubs.acs.org>.

JO051367V

(22) Gasparrini, F.; Pierini, M.; Villani, C.; De Maria, P.; Fontana, A.; Ballini, R. *J. Org. Chem.* **2003**, *68*, 3173.